



Analysis of false-positive and false-negative results in ^{99m}Tc -MIBI SPECT/CT parathyroid imaging

Yan Liu¹, Lulu Yang¹, Hui Xu¹, Yiyuan Yang¹, Yiqian Liang¹, Aimin Yang¹, Xiaojiang Tang², Shengkai Lei³, Ioannis Christakis⁴, Pornpeera Jitpratoom⁵, Jianjun Xue¹

¹Department of Nuclear Medicine, the First Affiliated Hospital of Xi'an Jiaotong University, Xi'an, China; ²Department of Breast Surgery, the First Affiliated Hospital of Xi'an Jiaotong University, Xi'an, China; ³Department of Internal Medicine, Hospital of Xi'an University of Architecture and Technology, Xi'an, China; ⁴Department of Endocrine Surgery, Nottingham University Hospitals NHS Trust, City Hospital, Nottingham, UK; ⁵Department of Surgery, Police General Hospital, Bangkok, Thailand

Contributions: (I) Conception and design: J Xue; (II) Administrative support: A Yang, J Xue; (III) Provision of study materials or patients: X Tang, Y Yang, S Lei; (IV) Collection and assembly of data: Y Liu, L Yang, H Xu, Y Yang; (V) Data analysis and interpretation: Y Liu, J Xue, Y Liang, A Yang; (VI) Manuscript writing: All authors; (VII) Final approval of manuscript: All authors.

Correspondence to: Jianjun Xue, MD, Department of Nuclear Medicine, the First Affiliated Hospital of Xi'an Jiaotong University, 277 West Yanta Road, Xi'an 710061, China. Email: xuejianjun@mail.xjtu.edu.cn.

Background: Exact preoperative localization is desirable to perform minimally invasive parathyroidectomy for hyperparathyroidism (HPT). This study aimed to evaluate the diagnostic values of ^{99m}Tc -methoxyisobutylisonitrile (^{99m}Tc -MIBI) single photon emission computed tomography/computed tomography (SPECT/CT) of parathyroid glands by analyzing the relationship between lesion weight and false-negative (FN) results, as well as to explain the possible reason.

Methods: The data from 314 patients with suspected HPT who underwent ^{99m}Tc -MIBI SPECT/CT parathyroid imaging between 2011 and 2022 were retrospectively evaluated. The sensitivity, positive predictive value (PPV), negative predictive value (NPV), and accuracy of parathyroid ^{99m}Tc -MIBI SPECT/CT were calculated, and the false-positive (FP) and FN findings were analyzed.

Results: Accurate localization by ^{99m}Tc -MIBI SPECT/CT was significantly associated with the parathyroid hormone (PTH) level. The ^{99m}Tc -MIBI SPECT/CT for diagnosis/lesion location reached a sensitivity of 84.6%/56.8%, a PPV of 97.3%/98.4%, an NPV of only 23.7%/4.18%, and an accuracy of 83.4%/57.1%, respectively. The largest diameter, shortest diameter, and lesion volume were lower in the FN group than in the TP group. A total of 7 FP cases were found, including 2 cases of thyroid nodules, 4 cases of thyroid tissue, and 1 case of hibernoma. A total of 45 FN patients, including 321 FN lesions, were confirmed, of which parathyroid hyperplasia accounted for 97.8%. Lesion weights greater than 20 μg were able to be detected, but lightweight lesions less than 100 mg were the principal source of FN results, accounting for approximately 39.3%. With lesion weights 0–100, 101–300, 301–1,000, and >1,000 mg, the FN rate was 70.8% (126/178), 51.8% (103/199), 34.6% (81/234), and 8.33% (11/132), respectively.

Conclusions: ^{99m}Tc -MIBI SPECT/CT parathyroid imaging provides good sensitivity and high specificity in HPT location. Correct localization by ^{99m}Tc -MIBI SPECT/CT correlates positively with lesion weight and PTH levels. The smaller the lesion, the higher the FN rate in ^{99m}Tc -MIBI SPECT/CT parathyroid imaging, and lesions weighing less than 100 mg are the main source of FN results in ^{99m}Tc -MIBI SPECT/CT parathyroid imaging.

Keywords: Hyperparathyroidism (HPT); single photon emission computed tomography/computed tomography (SPECT/CT); ^{99m}Tc -methoxyisobutylisonitrile (^{99m}Tc -MIBI); false-positive (FP); false-negative (FN)

Submitted Jul 31, 2023. Accepted for publication Oct 27, 2023. Published online Nov 06, 2023.

doi: 10.21037/qims-23-1091

View this article at: <https://dx.doi.org/10.21037/qims-23-1091>

Introduction

Hyperparathyroidism (HPT) is a common endocrine disorder that results from the autonomous overproduction of parathyroid hormone (PTH) by abnormal parathyroid glands (1). The diagnosis of HPT and its classification is primarily based on plasma biochemical profiling rather than imaging. Currently, the only definitive and gold-standard treatment for HPT is minimally invasive parathyroidectomy, requiring accurate pre-operative localization of the hyperfunctioning parathyroid gland (2,3). A number of diagnostic modalities can be used pre-operatively, including cervical ultrasound (US), 4-dimensional computed tomography (4DCT), and ^{18}F -fluorocholine positron emission tomography (PET) scans, with each one having different accuracy and characteristics (4,5). Cakal *et al.* reported that the sensitivity of cervical US was 89.7% and that of $^{99\text{m}}\text{Tc}$ -methoxyisobutylisonitrile ($^{99\text{m}}\text{Tc}$ -MIBI) was 71.8%, and their combined use had a sensitivity of 92.3% (6). Salhi *et al.* (7) reported that the positive predictive values (PPVs) of the above three imaging modalities for parathyroid adenomas were 97.6%, 97.7%, and 100%, respectively. Cervical US is widely accepted as one of the prescreening methods of choice for localization of HPT, followed by $^{99\text{m}}\text{Tc}$ -MIBI scintigraphy, because it is quick, economical, non-invasive, and a reasonably sensitive exam for patients. The role of magnetic resonance imaging (MRI) and multiphasic dynamic contrast-enhanced computed tomography (CT) imaging, termed 4DCT, has received increasing attention for HPT localization in recent years. However, their disadvantages include reliance on hemodynamic and vascular features, and they often display non-specific and variable reliability. Moreover, 4DCT induces high radiation exposure and the need for iodinated contrast medium (8), and the dose to the thyroid with 4DCT has been reported as about 57 times higher (92.0 *vs.* 1.6 mGy) than that with $^{99\text{m}}\text{Tc}$ -MIBI SPECT imaging (9). Currently, radionuclide imaging includes $^{99\text{m}}\text{Tc}$ -MIBI parathyroid scintigraphy and ^{18}F -fluorocholine PET. $^{99\text{m}}\text{Tc}$ -MIBI parathyroid scintigraphy includes double-tracer imaging subtraction techniques and single-tracer dual-phase imaging. Several studies have reported that

MIBI dual-phase parathyroid scintigraphy is an acceptable imaging method for localizing parathyroid adenoma and is superior to US, CT, and MRI (10-13). In recent years, most parathyroid scintigraphy has been performed in conjunction with single photon emission computed tomography/CT (SPECT/CT) to provide accurate 3-dimensional (3D) anatomical localization, superior to that of CT imaging (14). Previous studies have also reported that $^{99\text{m}}\text{Tc}$ -MIBI SPECT/CT parathyroid imaging showed higher sensitivity, accuracy, and PPV values for solitary parathyroid adenoma compared to cervical US or CT. A review of 24 studies including 1,276 patients using $^{99\text{m}}\text{Tc}$ -MIBI SPECT/CT between 2003 and 2014 showed that SPECT/CT was superior to SPECT and dual phase planar techniques for HPT localization, with a per-patient sensitivity of 86%, 74%, and 70%, respectively (14). Therefore, the $^{99\text{m}}\text{Tc}$ -MIBI SPECT/CT technique is among the preferred scintigraphic methods for localizing hyperfunctioning parathyroid glands, especially in ectopic locations (14), is the current standard method for detecting HPT (8), and is the conventional first-line presurgical imaging method (15)—often in conjunction with ultrasound—which is generally accepted. If the results of SPECT/CT parathyroid scintigraphy are equivocal or negative, an alternative investigation using a hybrid PET/CT technique is recommended (15). Recently published parathyroid imaging guidelines suggested that when possible, ^{18}F -fluorocholine PET/CT was a potential “alternative” first-line option for patients with primary HPT (8).

To date, investigations into the false-positive (FP) and false-negative (FN) rates of $^{99\text{m}}\text{Tc}$ -MIBI parathyroid scans have not been well documented, despite frequent cases being encountered in clinical practice. Exploring the factors that lead to unsatisfactory results is critical for lesion localization before parathyroidectomy. In this study, using postoperative pathological findings as the gold standard, we analyzed the results of $^{99\text{m}}\text{Tc}$ -MIBI SPECT/CT in order to highlight the factors influencing FPs and FNs and improve the preoperative localization of hyperfunctioning parathyroid glands. We present this article in accordance with the STARD reporting checklist (available at <https://qims.amegroups.com/article/view/10.21037/qims-23-1091/rc>).

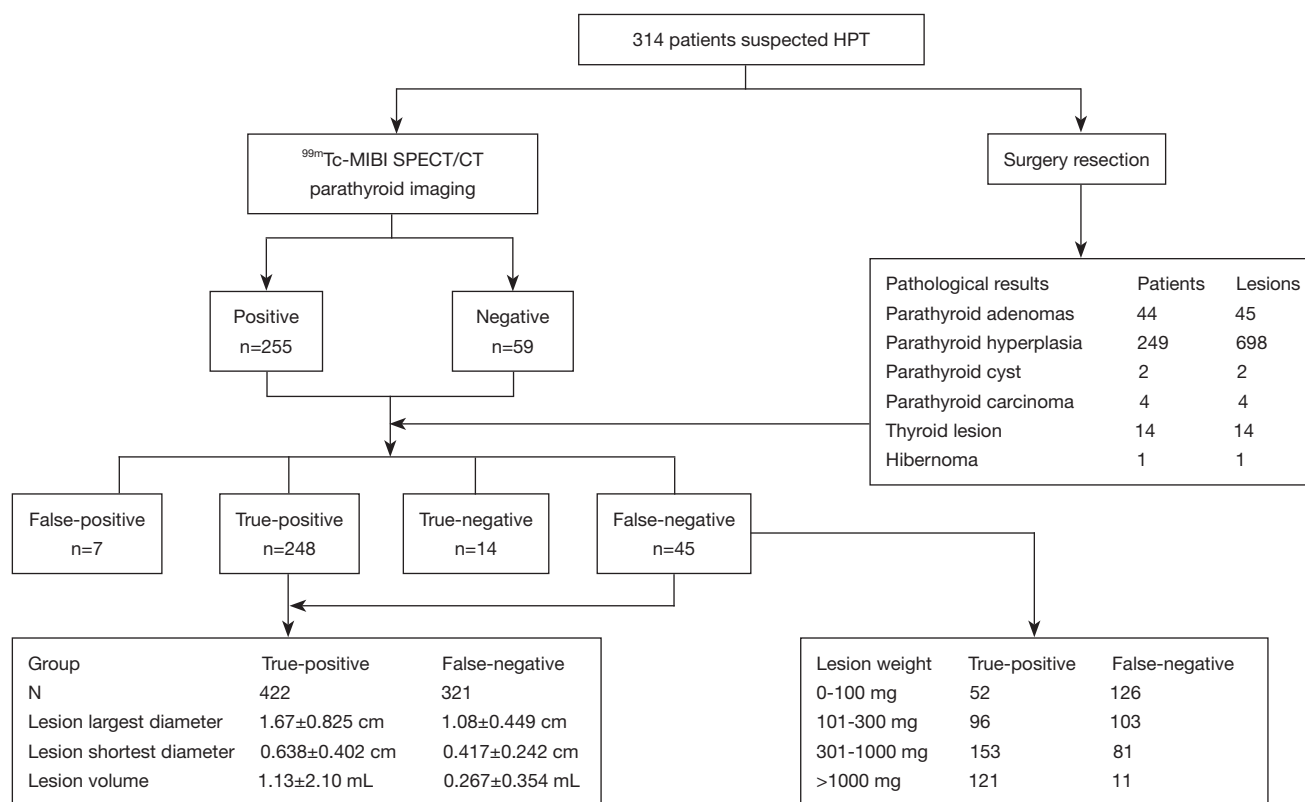


Figure 1 Study flowchart. HPT, hyperparathyroidism; ^{99m}Tc-MIBI, ^{99m}Tc-methoxyisobutylisonitrile; SPECT/CT, single photon emission computed tomography/computed tomography.

Methods

Participants

A total of 314 patients (162 women, 152 men; median age 47.2±13.1 years; range, 13–78 years) with biochemical evidence of suspected HPT and excluded multiple endocrine neoplasia 1 (MEN1) by other examination who underwent a parathyroidectomy at the First Affiliated Hospital of Xi’an Jiaotong University between 2011 and 2022 were included. Their data were analyzed retrospectively in this investigation (Figure 1). The female/male ratio was 1.07 (162 females vs. 152 males). All participants underwent parathyroid US and ^{99m}Tc-MIBI SPECT/CT examination for lesion positioning, and contrast enhanced CT examination of the neck and mediastinum was also conducted when ectopic parathyroid glands were suspected. When the surgeons could not identify the parathyroid lesions intraoperatively, if an initial diagnosis of secondary HPT had been made, intraoperative exploration and total parathyroidectomy with autotransplantation were performed mainly based on

the surgeon’s experience and exploration of the operative area. To confirm whether the parathyroid lesions had been effectively resected, serial serum PTH tests were performed from 20 minutes postoperatively. After parathyroidectomy, the width, length, and thickness of each lesion were recorded before histopathology examination, then the volume of the lesion was estimated according to the ellipsoid volume formula as follows: lesion volume (mL) = $\pi/6 \times \text{width (cm)} \times \text{length (cm)} \times \text{depth (cm)}$ (16). A previous study showed that the density of diseased parathyroid tissue is between 1.049 and 1.069 (17), so the lesion volume was assumed to represent lesion weight (1 mL = 1 gram). Serum PTH, lesion weight, diameter of HPT, and postoperative pathological data were collected from individual medical case records and reports. The study was conducted in accordance with the Declaration of Helsinki (as revised in 2013). The study was approved by the institutional review board of The First Affiliated Hospital of Xi’an Jiaotong University (No. XJTU1AF2021LSL-023, Xi’an, China), and the requirement for individual consent for this

Table 1 Pathological results of 314 patients who underwent ^{99m}Tc -MIBI SPECT/CT parathyroid imaging

Parameters	Patients	Lesions
Parathyroid adenomas	44	45
Parathyroid hyperplasia	249	698
Parathyroid cyst	2	2
Parathyroid carcinoma	4	4
Thyroid lesion	14	14
Hibernoma	1	1
Sum	314	764

^{99m}Tc -MIBI, ^{99m}Tc -methoxyisobutylisonitrile; SPECT/CT, single photon emission computed tomography/computed tomography.

retrospective analysis was waived.

^{99m}Tc -MIBI SPECT/CT

All patients underwent ^{99m}Tc -MIBI SPECT/CT before surgery by GE DiscoveryTM NM/CT 670 Pro SPECT/CT (GE Healthcare, Milwaukee, WI, USA). The acquisition conditions were as follows: low energy general collimator, peak of 140 KeV and the window width $\pm 20\%$, a 256 \times 256 matrix, and 60 projections were acquired over 360 $^\circ$ with an acquisition time of 20 seconds per view. Double-phase scintigraphy of the head, neck, and chest area in the anterior view was performed 15 minutes (early phase) and 120 minutes (delayed phase) after the intravenous injection of 740–1,110 MBq (20–30 mCi) of ^{99m}Tc -MIBI (Beijing Atom High Tech Co. Ltd., Beijing, China), with 500 k counts/view. The ^{99m}Tc -MIBI SPECT/CT was obtained 60 minutes after the ^{99m}Tc -MIBI injection.

Image analysis

The ^{99m}Tc -MIBI SPECT/CT images were interpreted independently by two experienced nuclear medicine physicians. To ensure the accuracy and reliability of the diagnostic results, any disputed results were judged by a third nuclear medicine practitioner, and the consensus results were used. Positive ^{99m}Tc -MIBI SPECT/CT double-phase scintigraphy used a radioactive focal concentration in the early phase and a fixed or increased concentration in the delayed phase.

Positive ^{99m}Tc -MIBI SPECT/CT lesions showed fixed tracer activities in parathyroid regions, extra parathyroid

regions of the neck, or mediastinum, and a soft tissue mass in the corresponding positions.

Judgment standard

TP was defined as a positive ^{99m}Tc -MIBI SPECT/CT image with postoperative pathology of parathyroid adenoma, hyperplasia, cyst or carcinoma; FP was defined as a positive ^{99m}Tc -MIBI SPECT/CT image with postoperative pathology of parathyroid gland; TN was defined as a negative ^{99m}Tc -MIBI SPECT/CT image with postoperative pathology of parathyroid gland; and FN was defined as a negative ^{99m}Tc -MIBI SPECT/CT image with postoperative pathology of parathyroid adenoma, hyperplasia, cyst, or carcinoma.

Statistical analysis

The data were analyzed using the software SPSS 18.0 (IBM Corp., Chicago, IL, USA). Continuous variables were expressed as the mean \pm standard deviation and were analyzed by independent-sample *t*-tests. The chi-square test was used to compare categorical variables. Statistical significance was set at $P < 0.05$.

Results

Pathological results

A total of 314 patients with suspected HPT underwent ^{99m}Tc -MIBI SPECT/CT parathyroid imaging and had reliable documentation of clinical outcomes. Among them, 135 underwent subtotal parathyroidectomy, and 179 underwent total parathyroidectomy with autotransplantation. A total of 764 masses were surgically removed and pathologically confirmed, and the pathological findings are summarized in *Table 1*.

^{99m}Tc -MIBI SPECT/CT parathyroid imaging

^{99m}Tc -MIBI SPECT/CT parathyroid imaging was TP in 248 patients, FP in 7 patients, FN in 45 patients, and TN in 14 patients. The demographic characteristics and PTH levels of the ^{99m}Tc -MIBI SPECT/CT parathyroid imaging are shown in *Table 2*. The PTH level in the positive group of ^{99m}Tc -MIBI SPECT/CT was significantly higher than that in the negative group ($t = 6.31$, $P < 0.001$). PTH levels were significantly different between the TN and FN

Table 2 Demographic characteristics and PTH levels of patients who underwent ^{99m}Tc -MIBI SPECT/CT ($\bar{x}\pm\text{SD}$)

Variables	Group 1				Group 2			
	True-positive	False-positive	χ^2 or t	P value	True-negative	False-negative	χ^2 or t	P value
Patients (n)	248	7	–	–	14	45	–	–
Female/male	119/129	4/3	0.009*	0.925	11/3	28/17	0.649*	0.421
Age (years)	47.2 \pm 13.4	45.0 \pm 14.9	0.420 [#]	0.675	44.6 \pm 12.1	48.4 \pm 11.6	1.06 [#]	0.295
PTH levels (pg/mL)	1476.2 \pm 1123.8	639.4 \pm 792.9	1.96 [#]	0.052	68.8 \pm 25.0	640.17 \pm 570.1	3.73 [#]	<0.001

*, chi-square test; [#], t -test. PTH, parathyroid hormone; ^{99m}Tc -MIBI, ^{99m}Tc -methoxyisobutylisonitrile; SPECT/CT, single photon emission computed tomography/computed tomography; SD, standard deviation.

Table 3 Results of ^{99m}Tc -MIBI SPECT/CT parathyroid imaging

Analysis	Sensitivity, % (n/N)	PPV, % (n/N)	NPV, % (n/N)	Accuracy, % (n/N)
Based on patient	84.6 (248/293)	97.3 (248/255)	23.7 (14/59)	83.4 (262/314)
Based on lesion	56.8 (422/743)	98.4 (422/429)	4.18 (14/335)	57.1 (436/764)

^{99m}Tc -MIBI, ^{99m}Tc -methoxyisobutylisonitrile; SPECT/CT, single photon emission computed tomography/computed tomography; PPV, positive predictive value; NPV, negative predictive value.

Table 4 Comparison of lesion size and volume in the true-positive and false-negative groups of ^{99m}Tc -MIBI SPECT/CT ($\bar{x}\pm\text{SD}$)

Variables	True-positive (n=422)	False-negative (n=321)	t	P value
Lesion largest diameter (cm)	1.67 \pm 0.83	1.08 \pm 0.45	11.5	<0.001
Lesion shortest diameter (cm)	0.64 \pm 0.40	0.42 \pm 0.24	8.74	<0.001
Lesion volume (mL)	1.13 \pm 2.10	0.27 \pm 0.35	7.30	<0.001

^{99m}Tc -MIBI, ^{99m}Tc -methoxyisobutylisonitrile; SPECT/CT, single photon emission computed tomography/computed tomography; SD, standard deviation.

groups, but not between the TP and FP groups of ^{99m}Tc -MIBI SPECT/CT. Based on patients/lesion locations respectively, the sensitivity of ^{99m}Tc -MIBI SPECT/CT reached 84.6%/56.8%, a PPV of 97.3%/98.4%, a negative predictive value (NPV) of 23.7%/4.18%, and an accuracy of 83.4%/57.1%, as summarized in *Table 3*. The largest diameter, shortest diameter, and lesion volume were lower in the FN group than in the TP group (*Table 4*).

FNs and FPs in ^{99m}Tc -MIBI SPECT/CT

A total of 7 FP cases were found, the pathological findings of which included 2 cases of thyroid nodules, 4 cases of thyroid tissue, and 1 case of hibernoma (*Figure 2*), respectively. A total of 45 and 321 FN results were identified based on patients and lesions, respectively (*Table 5*), which were parathyroid hyperplasia in about 97.8% (314/321),

mainly associated with multiglandular parathyroid disease (*Figure 3*). In addition, 3 parathyroid adenomas, 2 cysts, and 2 carcinomas were FN cases, which were single parathyroid lesions in 7 patients. Lesions weighing more than 20 μg could be detected, but lightweight lesions less than 100 mg were the principal source of FN results, accounting for about 39.3% (126/321). It was statistically significant that the smaller the lesion weight, the higher the FN rate (*Table 6*). There were 18 and 27 cases of primary HPT and secondary HPT, respectively, among the 45 FN cases, and 5 and 2 cases, respectively, among the 7 FP cases.

Discussion

HPT is a worldwide and common endocrine disorder characterized by persistent and excessive elevation of PTH, which often raises total serum calcium (Ca) levels

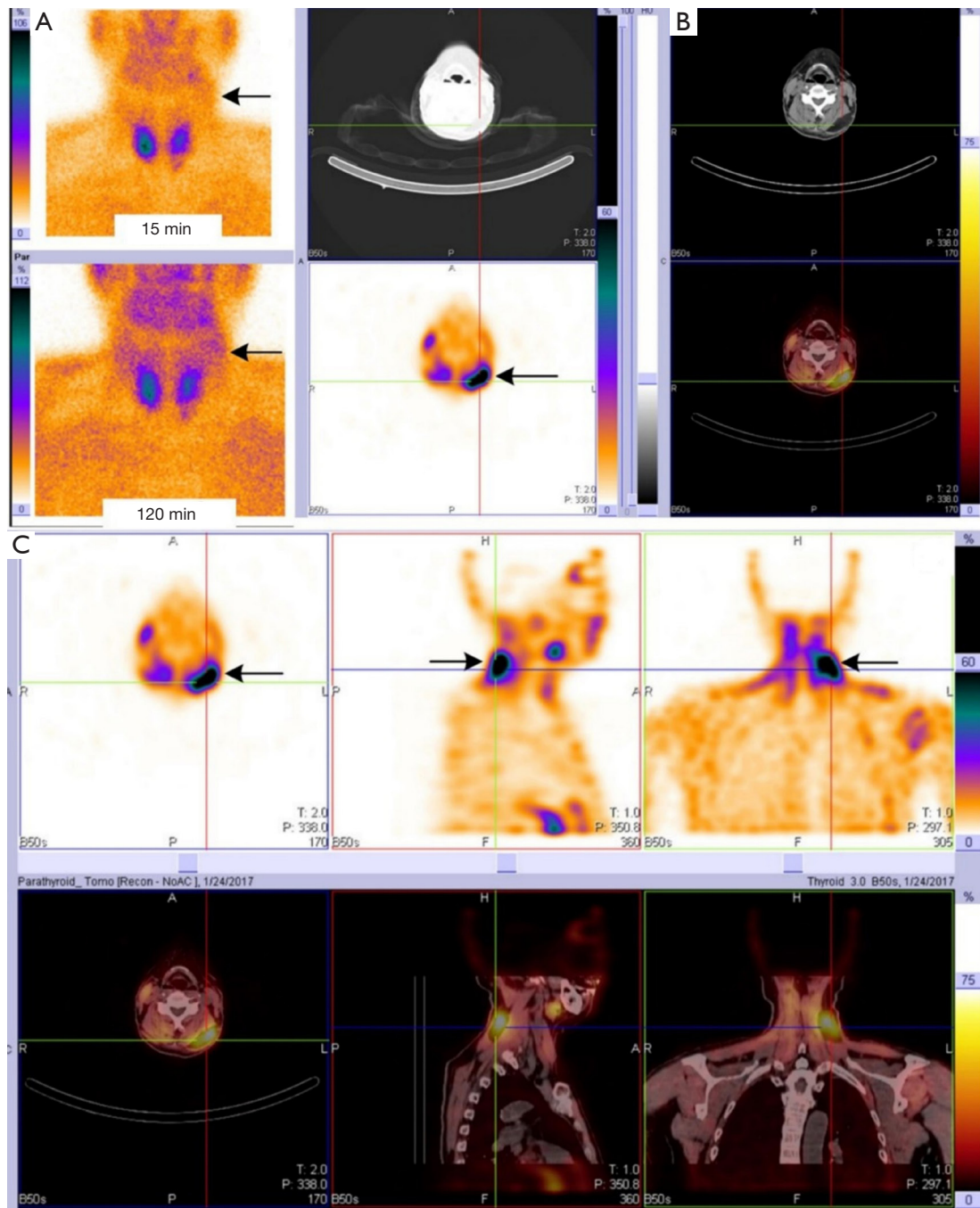


Figure 2 ^{99m}Tc -MIBI parathyroid imaging false-positive result. (A) ^{99m}Tc -MIBI planar imaging; (B,C) ^{99m}Tc -MIBI SPECT/CT parathyroid imaging. A 74-year-old patient diagnosed with primary HPT who underwent double-phase ^{99m}Tc -MIBI scintigraphy, and postoperative pathological findings show hibernoma. The image (anterior view, 15 and 120 min) shows mild focal tracer uptake in the left neck (arrows). Neck ultrasonography shows a hyperechoic nodule lesion measuring $53 \times 15 \times 50 \text{ mm}^3$ in the posterior portion of the left neck. Transaxial ^{99m}Tc -MIBI SPECT/CT fusion image (B,C) (60 min after injection) shows abnormal focal concentration in the left neck (arrows) Hibernoma is a rare benign tumor and contains abundant mitochondria that are highly active metabolically, leading to intense ^{99m}Tc -MIBI accumulation. ^{99m}Tc -MIBI, ^{99m}Tc -methoxyisobutylisonitrile; SPECT/CT, single photon emission computed tomography/computed tomography.

Table 5 Results of false-negative in ^{99m}Tc -MIBI SPECT/CT

False-negative lesions	Patients, n (%)	Lesions, n (%)
Parathyroid hyperplasia	38 (84.4)	314 (97.8)
Parathyroid adenoma	3 (6.67)	3 (0.94)
Parathyroid cyst	2 (4.44)	2 (0.62)
Parathyroid carcinoma	2 (4.44)	2 (0.62)
Sum	45 (100.0)	321 (100.0)

^{99m}Tc -MIBI, ^{99m}Tc -methoxyisobutylisonitrile; SPECT/CT, single photon emission computed tomography/computed tomography.

in blood circulation. Clinically, PTH levels and serum Ca concentrations are always required for the initial diagnosis, and about 80% of cases can be identified with this information. The only definitive treatment of HPT is parathyroidectomy, so the importance of preoperative positioning cannot be overemphasized in helping to minimize the extent of dissection/exploration required.

Usually, the preoperative imaging choices are scintigraphy, high-resolution ultrasonography, CT scan, and

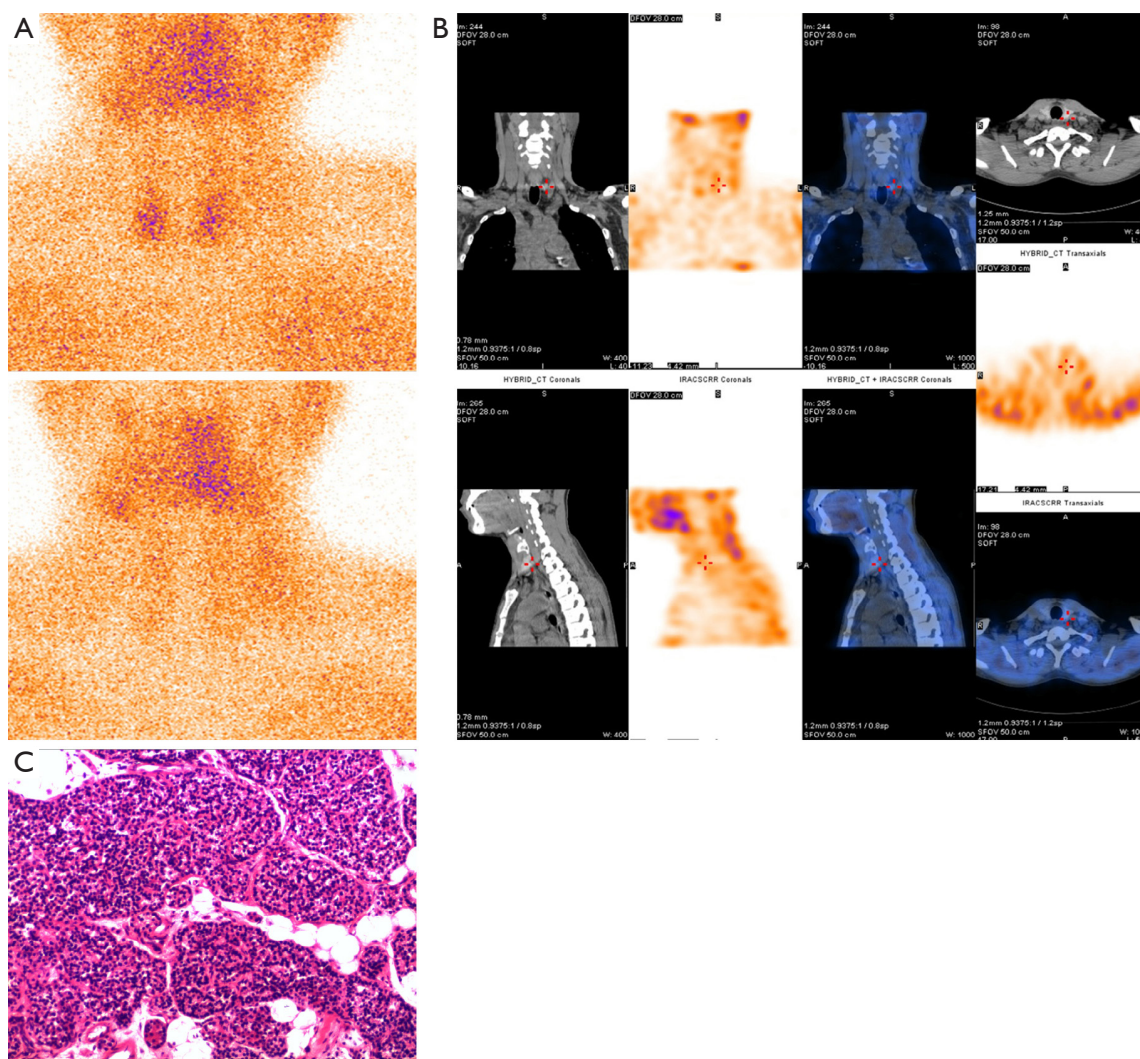


Figure 3 ^{99m}Tc -MIBI parathyroid imaging false-negative result. (A) ^{99m}Tc -MIBI planar imaging; (B) the false-negative of ^{99m}Tc -MIBI SPECT/CT parathyroid imaging; (C) postoperative pathological findings. A 43-year-old male patient repeatedly presented with high serum PTH (1,023.0 pg/mL) for several months on examinations. ^{99m}Tc -MIBI SPECT/CT parathyroid imaging shows no obvious hyperactivity of parathyroid tissue (A,B), and postoperative pathological findings show adenomatous hyperplasia of the parathyroid glands in the left upper, left lower, right upper, and right lower gland (C, HE staining, $\times 100$). ^{99m}Tc -MIBI, ^{99m}Tc -methoxyisobutylisonitrile; SPECT/CT, single photon emission computed tomography/computed tomography; PTH, parathyroid hormone; HE, hematoxylin and eosin.

Table 6 The relationship between the ^{99m}Tc -MIBI SPECT/CT false-negative rate and the total false-negative rate in different groups of lesion weight

Lesion weight (mg)	True-positive (n)	False-negative (n)	False-negative rate in ^{99m}Tc -MIBI SPECT/CT, % (n/N)	χ^2	P value
0–100	52	126	70.8 (126/178)	42.6	<0.001*
101–300	96	103	51.8 (103/199)	4.30	0.038*
301–1,000	153	81	34.6 (81/234)	5.07	0.024*
>1,000	121	11	8.3 (11/132)	56.4	<0.001*
Sum	422	321	43.2 (321/743)	–	–

*, $P < 0.05$, each group compared to the sum. ^{99m}Tc -MIBI, ^{99m}Tc -methoxyisobutylisonitrile; SPECT/CT, single photon emission computed tomography/computed tomography.

MRI (18), wherein ^{99m}Tc -MIBI scintigraphy plays an important role and is the first line imaging procedure to identify suitable patients undergoing parathyroidectomy (19). ^{99m}Tc -MIBI SPECT/CT parathyroid scintigraphy combines the functional glandular tissue abnormalities and the anatomical information, which is far more sensitive and accurate than the planar or the SPECT scintigraphic techniques in the preoperative localization of HPT lesions (20). Our data identified that the PPV of ^{99m}Tc -MIBI SPECT/CT was 98.6%, which is consistent with values reported by a meta-analysis based on 18 articles from the last 25 years; according to the report, the sensitivities of ^{99m}Tc -MIBI SPECT/CT, SPECT, and planar scintigraphy were 84% [95% confidence interval (CI): 78–90%], 66% (95% CI: 57–74%), and 63% (95% CI: 51–74%), respectively, and the corresponding PPVs were 95% (95% CI: 92–98%), 82% (95% CI: 73–89%), and 90% (95% CI: 96–99%), respectively (20). Therefore, ^{99m}Tc -MIBI SPECT/CT parathyroid imaging has a very high localization value for HPT, and positive imaging can provide valuable guidance for parathyroidectomy.

Previous studies on detection rates in ^{99m}Tc -MIBI parathyroid imaging have yielded heterogeneous results because some statistics have been based on lesion detection, and others have been based on patient diagnosis. Patients with parathyroid hyperplasia may have multiple lesions, and our previous study showed that a patient with parathyroid hyperplasia had an average of 2.96 lesions (21), which was the main reason for the important difference between the sensitivity and accuracy of the technique on patient-based and lesion-based analysis in Table 3. Therefore, the sensitivity and accuracy of a lesion-based analysis may better reflect the clinical value than those on a patient-based analysis. To better investigate the causes of FP and

FN lesions, this study examined the detection rates of both patient diagnoses and lesions. Our study showed a FP rate, based on patients, of 2.75% (7/255). The mechanism of ^{99m}Tc -MIBI uptake in the cell has been reported to be related to the mitochondria-rich oxyphilic cells in parathyroid adenomas (22,23), thyroid tissue, or thyroid nodules, which may be the main reason for FPs. Hibernoma is a rare benign tumor with an unclear etiology, with only 100 cases reported worldwide (24), and to our knowledge, there is no report that hibernoma can be detected by ^{99m}Tc -MIBI scintigraphy. Hibernoma contains abundant mitochondria (25,26), leading to intense ^{99m}Tc -MIBI accumulation. Other research has also found that hibernomas usually show increased F-18 fluoro-2-deoxy-d-glucose uptake because of their high metabolic level rather than from tumor growth activity (27).

Single parathyroid adenoma is the most common cause of HPT, observed in 80% of patients. The likely cause of HPT is multiglandular as adenomas or hyperplasias in 15% of patients, and it is rarely caused by malignant carcinoma (0.5–4% of cases) (28). However, in this study, the proportion of parathyroid hyperplasia was higher than that of adenoma, which is different from general epidemiology. The probable reason for this is that in clinical practice, when a single parathyroid adenoma is suspected, it is usually treated directly with surgery. In our study, parathyroid hyperplasia was most commonly associated with ^{99m}Tc -MIBI FN cases, and FNs in secondary HPT were more common than in primary HPT. The reason is that secondary HPT was predominantly multiple lesions, whereas primary HPT was predominantly single lesions. Tang *et al.* reported that the sensitivity of MIBI SPECT was 95% for adenoma and 59% for hyperplasia (29) because hyperplasia is more likely to be multiglandular disease than adenoma. Hyperplastic

parathyroid glands are usually smaller than adenoma, causing decreased sensitivity of MIBI imaging (30). Previous studies have demonstrated that in cases of very small HPT glands, FN results might occur with scintigraphy, which is in accordance with our findings. As shown in *Table 4*, the mean largest lesion diameter, shortest lesion diameter, and lesion volume (weight) in the TP group were 1.67 ± 0.83 cm, 0.64 ± 0.40 cm, and 1.13 ± 2.10 mL (mg), versus 1.08 ± 0.45 cm, 0.42 ± 0.24 cm, and 0.27 ± 0.35 mL (mg) in the FN group, respectively, and these differences were significant. The correlation between lesion size or weight and SPECT/CT detectability has been observed in previous reports (31,32). Gimlette *et al.* (31) reported that deeply located and lighter-weight parathyroid adenomas were more likely to be FNs on scintigraphy and that parathyroid adenomas should weigh at least 300 mg for location by thallium-201 scintigraphy. Hayakawa *et al.* further reported that MIBI SPECT/CT could only detect 1 out of 8 lesions smaller than 276 μ L (13%); in contrast, 9 out of 10 lesions equal to or larger than 276 μ L (90%) were detected (30). However, in our study, 69.5% (148/213) of lesions less than 300 mg were detected by ^{99m}Tc -MIBI SPECT/CT parathyroid imaging. The total FN rate of ^{99m}Tc -MIBI SPECT/CT in our study was 43.2% (321/743), which is far from satisfactory, but it was obvious that with the increase in lesion weight, the FN rate decreased. In fact, our results show that with lesion weights of 0–100, 101–300, 301–1,000, and >1,000 mg, the FN rate was 70.8% (126/178), 51.8% (103/199), 34.6% (81/234), and 8.33% (11/132), respectively. In our series, lesion size was the main reason for the FN results in ^{99m}Tc -MIBI SPECT/CT parathyroid imaging, which had higher accuracy than planar mode or SPECT mode scintigraphy without CT. Surprisingly, and contrary to previous reports, we found in this study that HPT lesions weighing at least 20 μ g could be detected by ^{99m}Tc -MIBI SPECT/CT, which is smaller than the mean weight of 40 mg of a normal parathyroid gland (19). We can reaffirm that the ^{99m}Tc -MIBI uptake by abnormal parathyroid glands is related to the functional activity of oxyphil cells, and not the cellularity weight of the glands.

The main pathological type of primary HPT is adenoma, whereas that of secondary HPT is hyperplasia. In our previous series, we investigated the localization value of ^{99m}Tc -MIBI SPECT/CT parathyroid imaging for primary and secondary HPT. Our findings revealed that overexpression of P-glycoprotein or multidrug resistance-associated protein-1 could result in an efflux of ^{99m}Tc -MIBI from tumor cells and lead to FN results in dual-phase

^{99m}Tc -MIBI imaging (32), which led to the conclusion that the sensitivity of early ^{99m}Tc -MIBI dual-phase scintigraphy imaging could be higher than that of delayed imaging (10,32,33). To maintain consistency with previous studies and to later reveal the possible mechanism of FP or FN parathyroid imaging, this study correlated ^{99m}Tc -MIBI SPECT/CT parathyroid imaging with pathological findings rather than with clinical diagnosis. ^{99m}Tc -MIBI uptake has also been linked to increased concentrations of mitochondria-rich oxyphil cells (34,35). Several other factors, including serum Ca, PTH level, blood flow, and MIBI biokinetics of the lesion, together with the secretory function and activity of the parathyroid cells, may influence lesion detectability in parathyroid scintigraphy (21,36). Some drugs, such as non-steroidal anti-inflammatory drugs (NSAIDs) and Ca channel blockers, also affect the sensitivity of ^{99m}Tc -MIBI SPECT, and the sensitivity of ^{99m}Tc -MIBI dual-phase parathyroid SPECT decreased from 96.5% to 75% by NSAIDs therapy (37). Research has shown that PTH levels are closely related to the detection rate of ^{99m}Tc -MIBI imaging (38). Durmuş *et al.* reported that among the biochemical variables, only PTH level was found to be significantly increased in the ^{99m}Tc -MIBI imaging -positive group (39). Blanco-Saiz *et al.* reported that the only factor significantly related to the sensitivity of MIBI SPECT/CT was the weight of the gland (40). PTH levels are strongly correlated with the detection rate of MIBI imaging, which has been confirmed by previous research and supported by this study. However, there was no significant difference in PTH levels between the TP and FP MIBI imaging groups in this study (*Table 2*). The reason may be that the number of FP cases was only 7, which is not enough for reliable statistical analysis or to be taken seriously; analysis in a larger group is required to obtain robust scientific results.

There were several limitations to this study. First, it used a nonrandomized, single-center, retrospective design. Second, the sample size of the study was small, and generalizability might be limited; when the surgeons could not identify the parathyroid lesions intraoperatively, parathyroidectomy was performed mainly based on the surgeon's experience and exploration of the operative area. Finally, studies have shown that the percentage of oxyphil cells is a very important factor in positive ^{99m}Tc -MIBI imaging. Unfortunately, the percentage of oxyphil cells was not available in the pathology, which is also a limitation of this study. Ince *et al.* reported that although there was no statistically significant difference according to cell type,

the content of chief cells and oxyphilic cells in parathyroid adenomas tended to decrease in negative or equivocal parathyroid scintigraphy, whereas the clear cell rate increased (41). This may mechanistically reveal the reason of FN MIBI imaging and should be given more attention in future.

Conclusions

Our study indicated that ^{99m}Tc -MIBI SPECT/CT parathyroid imaging provided good sensitivity and high specificity in HPT localization; lesions weighing at least 20 μg could be detected by ^{99m}Tc -MIBI SPECT/CT, in regard to the hyperfunctional activity of parathyroid cells. Correct localization by ^{99m}Tc -MIBI SPECT/CT correlated positively with lesion weight/size; the smaller the lesion, the higher the FN rate, and lesions weighing less than 100 mg were the main source of FN results in ^{99m}Tc -MIBI SPECT/CT parathyroid imaging.

Acknowledgments

Funding: This study was supported by the Clinical Research of the First Affiliated Hospital of Xi'an Jiaotong University, China (No. XJTU1AF2021CRF-024).

Footnote

Reporting Checklist: The authors have completed the STARD reporting checklist. Available at <https://qims.amegroups.com/article/view/10.21037/qims-23-1091/rc>

Conflicts of Interest: All authors have completed the ICMJE uniform disclosure form (available at <https://qims.amegroups.com/article/view/10.21037/qims-23-1091/coif>). The authors have no conflicts of interest to declare.

Ethical Statement: The authors are accountable for all aspects of the work in ensuring that questions related to the accuracy or integrity of any part of the work are appropriately investigated and resolved. The study was conducted in accordance with the Declaration of Helsinki (as revised in 2013). The study was approved by the institutional review board at The First Affiliated Hospital of Xi'an Jiaotong University (No. XJTU1AF2021LSL-023, Xi'an, China), and the requirement for individual consent for this retrospective analysis was waived.

Open Access Statement: This is an Open Access article distributed in accordance with the Creative Commons Attribution-NonCommercial-NoDerivs 4.0 International License (CC BY-NC-ND 4.0), which permits the non-commercial replication and distribution of the article with the strict proviso that no changes or edits are made and the original work is properly cited (including links to both the formal publication through the relevant DOI and the license). See: <https://creativecommons.org/licenses/by-nc-nd/4.0/>.

References

1. Wilhelm SM, Wang TS, Ruan DT, Lee JA, Asa SL, Duh QY, Doherty GM, Herrera MF, Pasiaka JL, Perrier ND, Silverberg SJ, Solórzano CC, Sturgeon C, Tublin ME, Udelsman R, Carty SE. The American Association of Endocrine Surgeons Guidelines for Definitive Management of Primary Hyperparathyroidism. *JAMA Surg* 2016;151:959-68.
2. Andersen TB, Aleksyniene R, Boldsen SK, Gade M, Bertelsen H, Petersen LJ. Contrast-enhanced computed tomography does not improve the diagnostic value of parathyroid dual-phase MIBI SPECT/CT. *Nucl Med Commun* 2018;39:435-40.
3. Morris MA, Saboury B, Ahlman M, Malayeri AA, Jones EC, Chen CC, Millo C. Parathyroid Imaging: Past, Present, and Future. *Front Endocrinol (Lausanne)* 2021;12:760419.
4. Christakis I, Vu T, Chuang HH, Fellman B, Figueroa AMS, Williams MD, Busaidy NL, Perrier ND. The diagnostic accuracy of neck ultrasound, 4D-Computed tomography and sestamibi imaging in parathyroid carcinoma. *Eur J Radiol* 2017;95:82-8.
5. Christakis I, Khan S, Sadler GP, Gleeson FV, Bradley KM, Mihai R. (18)Fluorocholine PET/CT scanning with arterial phase-enhanced CT is useful for persistent/recurrent primary hyperparathyroidism: first UK case series results. *Ann R Coll Surg Engl* 2019;101:501-7.
6. Cakal E, Cakir E, Dilli A, Colak N, Unsal I, Aslan MS, Karbek B, Ozbek M, Kilic M, Delibasi T, Sahin M. Parathyroid adenoma screening efficacies of different imaging tools and factors affecting the success rates. *Clin Imaging* 2012;36:688-94.
7. Salhi H, Bouziane T, Maaroufi M, Alaoui NI, El Ouahabi H. Primary hyperparathyroidism: Correlation between cervical ultrasound and MIBI scan. *Ann Afr Med* 2022;21:161-4.

8. Petranović Ovcariček P, Giovanella L, Carrió Gasset I, Hindié E, Huellner MW, Luster M, Piccardo A, Weber T, Talbot JN, Verburg FA. The EANM practice guidelines for parathyroid imaging. *Eur J Nucl Med Mol Imaging* 2021;48:2801-22.
9. Mahajan A, Starker LF, Ghita M, Udelsman R, Brink JA, Carling T. Parathyroid four-dimensional computed tomography: evaluation of radiation dose exposure during preoperative localization of parathyroid tumors in primary hyperparathyroidism. *World J Surg* 2012;36:1335-9.
10. Mariani G, Gulec SA, Rubello D, Boni G, Puccini M, Pelizzo MR, Manca G, Casara D, Sotti G, Erba P, Volterrani D, Giuliano AE. Preoperative localization and radioguided parathyroid surgery. *J Nucl Med* 2003;44:1443-58.
11. Palestro CJ, Tomas MB, Tronco GG. Radionuclide imaging of the parathyroid glands. *Semin Nucl Med* 2005;35:266-76.
12. Dackiw AP, Sussman JJ, Fritsche HA Jr, Delpassand ES, Stanford P, Hoff A, Gagel RF, Evans DB, Lee JE. Relative contributions of technetium Tc 99m sestamibi scintigraphy, intraoperative gamma probe detection, and the rapid parathyroid hormone assay to the surgical management of hyperparathyroidism. *Arch Surg* 2000;135:550-5; discussion 555-7.
13. Siegel A, Alvarado M, Barth RJ Jr, Brady M, Lewis J. Parameters in the prediction of the sensitivity of parathyroid scanning. *Clin Nucl Med* 2006;31:679-82.
14. Wong KK, Fig LM, Gross MD, Dwamena BA. Parathyroid adenoma localization with 99mTc-sestamibi SPECT/CT: a meta-analysis. *Nucl Med Commun* 2015;36:363-75.
15. Mathey C, Keyzer C, Blocklet D, Van Simaey G, Trotta N, Lacroix S, Corvilain B, Goldman S, Moreno-Reyes R. (18)F-Fluorocholine PET/CT Is More Sensitive Than (11)C-Methionine PET/CT for the Localization of Hyperfunctioning Parathyroid Tissue in Primary Hyperparathyroidism. *J Nucl Med* 2022;63:785-91.
16. Gupta Y, Ahmed R, Happerfield L, Pinder SE, Balan KK, Wishart GC. P-glycoprotein expression is associated with sestamibi washout in primary hyperparathyroidism. *Br J Surg* 2007;94:1491-5.
17. Wang CA, Rieder SV. A density test for the intraoperative differentiation of parathyroid hyperplasia from neoplasia. *Ann Surg* 1978;187:63-7.
18. Williams MD, DeLellis RA, Erickson LA, Gupta R, Johnson SJ, Kameyama K, Natu S, Ng T, Perren A, Perrier ND, Seethala RR, Gill AJ. Pathology data set for reporting parathyroid carcinoma and atypical parathyroid neoplasm: recommendations from the International Collaboration on Cancer Reporting. *Hum Pathol* 2021;110:73-82.
19. Kowalski G, Buła G, Bednarczyk A, Gawrychowska A, Gawrychowski J. *Multiglandular Parathyroid Disease*. Life (Basel) 2022.
20. Wei WJ, Shen CT, Song HJ, Qiu ZL, Luo QY. Comparison of SPET/CT, SPET and planar imaging using 99mTc-MIBI as independent techniques to support minimally invasive parathyroidectomy in primary hyperparathyroidism: A meta-analysis. *Hell J Nucl Med* 2015;18:127-35.
21. Xue J, Liu Y, Ji T, Zhao A, Liang Y, Deng H, Wang Q, Zhang Y, Yang L, Yang A. Comparison between technetium-99m methoxyisobutylisonitrile scintigraphy and ultrasound in the diagnosis of parathyroid adenoma and parathyroid hyperplasia. *Nucl Med Commun* 2018;39:1129-37.
22. Bénard F, Lefebvre B, Beuvon F, Langlois MF, Bisson G. Rapid washout of technetium-99m-MIBI from a large parathyroid adenoma. *J Nucl Med* 1995;36:241-3.
23. Piñero A, Rodríguez JM, Martínez-Barba E, Canteras M, Stiges-Serra A, Parrilla P. Tc99m-sestamibi scintigraphy and cell proliferation in primary hyperparathyroidism: a causal or casual relationship? *Surgery* 2003;134:41-4.
24. Saito M, Tsuji Y, Murata H, Kanemitsu K, Makinodan A, Ikeda T, Konishi E, Kubo T. Hibernoma of the right back. *Orthopedics* 2007;30:495-6.
25. Subramaniam RM, Clayton AC, Karantanis D, Collins DA. Hibernoma: 18F FDG PET/CT imaging. *J Thorac Oncol* 2007;2:569-70.
26. Botchu R, Puls F, Hock YL, Davies AM, Wafa H, Grimer RJ, Bröcker V, James S. Intraosseous hibernoma: a case report and review of the literature. *Skeletal Radiol* 2013;42:1003-5.
27. Tsuchiya T, Osanai T, Ishikawa A, Kato N, Watanabe Y, Ogino T. Hibernomas show intense accumulation of FDG positron emission tomography. *J Comput Assist Tomogr* 2006;30:333-6.
28. Yeh MW, Ituarte PH, Zhou HC, Nishimoto S, Liu IL, Harari A, Haigh PI, Adams AL. Incidence and prevalence of primary hyperparathyroidism in a racially mixed population. *J Clin Endocrinol Metab* 2013;98:1122-9.
29. Tang BN, Moreno-Reyes R, Blocklet D, Corvilain B, Cappello M, Delpierre I, Devuyst F, Van Simaey G, Goldman S. Accurate pre-operative localization of pathological parathyroid glands using 11C-methionine PET/CT. *Contrast Media Mol Imaging* 2008;3:157-63.

30. Hayakawa N, Nakamoto Y, Kurihara K, Yasoda A, Kanamoto N, Miura M, Inagaki N, Togashi K. A comparison between ¹¹C-methionine PET/CT and MIBI SPECT/CT for localization of parathyroid adenomas/hyperplasia. *Nucl Med Commun* 2015;36:53-9.
31. Gimlette TM, Brownless SM, Taylor WH, Shields R, Simkin EP. Limits to parathyroid imaging with thallium-201 confirmed by tissue uptake and phantom studies. *J Nucl Med* 1986;27:1262-5.
32. Xue J, Liu Y, Yang D, Yu Y, Geng Q, Ji T, Yang L, Wang Q, Wang Y, Lu X, Yang A. Dual-phase ^{99m}Tc-MIBI imaging and the expressions of P-gp, GST- π , and MRP1 in hyperparathyroidism. *Nucl Med Commun* 2017;38:868-74.
33. Lorberboym M, Minski I, Macadziob S, Nikolov G, Schachter P. Incremental diagnostic value of preoperative ^{99m}Tc-MIBI SPECT in patients with a parathyroid adenoma. *J Nucl Med* 2003;44:904-8.
34. Pons F, Torregrosa JV, Fuster D. Biological factors influencing parathyroid localization. *Nucl Med Commun* 2003;24:121-4.
35. Melloul M, Paz A, Koren R, Cytron S, Feinmesser R, Gal R. ^{99m}Tc-MIBI scintigraphy of parathyroid adenomas and its relation to tumour size and oxyphil cell abundance. *Eur J Nucl Med* 2001;28:209-13.
36. Gungor S, Dede F, Can B, Keskin H, Aras M, Ones T, Erdil TY, Turoglu HT. The value of parathyroid scintigraphy on lesion detection in patients with normocalcemic primary hyperparathyroidism. *Rev Esp Med Nucl Imagen Mol (Engl Ed)* 2022;41:86-90.
37. Araz M, Çayır D, Erdoğan M, Uçan B, Çakal E. Factors affecting the sensitivity of Tc-^{99m} methoxyisobutylisonitrile dual-phase parathyroid single photon emission computed tomography in primary hyperparathyroidism. *Nucl Med Commun* 2017;38:117-23.
38. Carral F, Jiménez AI, Tomé M, Álvarez J, Díez A, Partida F, Ayala C. Factors associated with negative (^{99m}Tc-MIBI scanning in patients with primary hyperparathyroidism. *Rev Esp Med Nucl Imagen Mol (Engl Ed)* 2021;40:222-8.
39. Durmuş ET, Atmaca A, Kefeli M, Mete Ö, Canbaz Tosun F, Bayçebebi D, Polat C, Çolak R. Clinicopathological variables that correlate with sestamibi positivity in uniglandular parathyroid disease: a retrospective analysis of 378 parathyroid adenomas. *Ann Nucl Med* 2022;36:33-42.
40. Blanco-Saiz I, Goñi-Gironés E, Ribelles-Segura MJ, Salvador-Egea P, Díaz-Tobarrá M, Camarero-Salazar A, Rudic-Chipe N, Saura-López I, Alomar-Casanovas A, Rabines-Juárez A, García-Torres J, Anda-Apiñániz E. Preoperative parathyroid localization. Relevance of MIBI SPECT-CT in adverse scenarios. *Endocrinol Diabetes Nutr (Engl Ed)* 2023;70 Suppl 2:35-44.
41. Ince S, Emer O, Deveci S, Okuyucu K, Alagoz E, San H, Ayan A, Karacalioglu O, Haymana C, Gunalp B, Arslan N. Complementary role of parathormone washout test to (^{99m}Tc-MIBI parathyroid scintigraphy and histopathologic analysis of cell types in parathyroid adenomas. *Rev Esp Med Nucl Imagen Mol (Engl Ed)* 2018;37:205-10.

Cite this article as: Liu Y, Yang L, Xu H, Yang Y, Liang Y, Yang A, Tang X, Lei S, Christakis I, Jitpratoom P, Xue J. Analysis of false-positive and false-negative results in ^{99m}Tc-MIBI SPECT/CT parathyroid imaging. *Quant Imaging Med Surg* 2023;13(12):8669-8680. doi: 10.21037/qims-23-1091